

Performances of X-shooter, the new wide band intermediate resolution spectrograph at the VLT

J. Vernet^a, H. Dekker^a, S. D'Odorico^a, E. Mason^a, P. Di Marcantonio^b, M. Downing^a, E. Elswijk^c, G. Finger^a, G. Fischer^a, F. Kerber^a, L. Kern^a, J.-L. Lizon^a, C. Lucuix^a, V. Mainieri^a, A. Modigliani^a, F. Patat^a, S. Ramsay^a, P. Santin^b, M. Vidali^d, P. Groot^e, I. Guinouard^f, F. Hammer^f, L. Kaper^g, P. Kjaergaard-Rasmussen^h, R. Navarro^c, S. Randichⁱ, F. Zerbi^j

^aEuropean Southern Observatory, Karl Schwarzschild Str. 2, 85748 Garching bei Muenchen, Germany;

^bINAF Osservatorio di Trieste, Via Tiepolo 11, 34143 Trieste, Italy;

^cASTRON - NOVA, Oude Hoogeveensedijk 4 7991 PD Dwingeloo, The Netherlands;

^dEC JRC Institute for Reference Materials and Measurements, B-2440 Geel, Belgium;

^eRadboud Univ. Nijmegen, Postbus 9010, 6500 GL Nijmegen, The Netherlands;

^fGEPI - Observatoire de Paris, 5 place Jules Janssen, F-92195 Meudon, France;

^gAstronomical Institute Anton Pannekoek, Univ. of Amsterdam, Postbus 19268, 1000 GG Amsterdam, The Netherlands;

^hNiels Bohr Institute for Astronomy, Niels Bohr Institute for Astronomy, Blegdamsvej 17, DK-2100 Copenhagen, Denmark;

ⁱINAF-Osservatorio di Arcetri, Largo E. Fermi, 50125 Firenze, Italy;

^jINAF-Osservatorio di Brera, Via E. Bianchi 46, 23807 Merate, Italy

ABSTRACT

X-shooter is the first second-generation instrument newly commissioned at the VLT. It is a high efficiency single target intermediate resolution spectrograph covering the range 300 - 2500 nm in a single shot. We summarize the main characteristics of the instrument and present its performances as measured during commissioning and the first months of science operations.

Keywords: X-shooter, VLT, performance

1. INTRODUCTION

X-shooter is the first 2nd generation VLT instrument and replaces at the Cassegrain focus of the Kueyen telescope (UT2) the workhorse-instrument FORS1, after more than a decade of successful operations. This unique instrument collects simultaneously the full spectrum of a single target from 300 to 2500 nm at a spectral resolution varying between 3,000 and 17,000 depending on the slit width and the wavelength. It consists of a central structure (backbone), which supports three prism-cross-dispersed chelle spectrographs optimized for the UV-Blue (UVB), Visible (VIS) and Near-IR (NIR) wavelength ranges respectively. At the entrance of each spectrograph there is a slit unit, equipped with 11 arcsec long slits of different width. After the focus, two highly efficient dichroics in series reflect the UVB and VIS light to the corresponding arms and transmit longer wavelengths to the NIR arm. A slicer can be inserted in the focal plane, which reformat 1.8×4 arcsec on the sky into a 0.6×12 arcsec long slit. A functional diagram of the instrument is given in Fig. 1.

After two commissioning runs with the UVB and VIS arms only in November 2008 and January 2009, the instrument reached its full configuration in March 2009 (see Fig. 1) and has been in science operations since October 2009. It has lived up to expectations in terms of image quality, spectral resolution and simple and robust operation. The possibility to collect the full spectrum from the atmospheric UV cutoff to the K band at intermediate resolution in a single shot is an attractive option for a variety of scientific programs, from the study of solar system bodies to the search of emission galaxies at high redshift. In the first two Calls where it was offered for general use X-shooter has been the second most requested instrument at the VLT (after FORS).

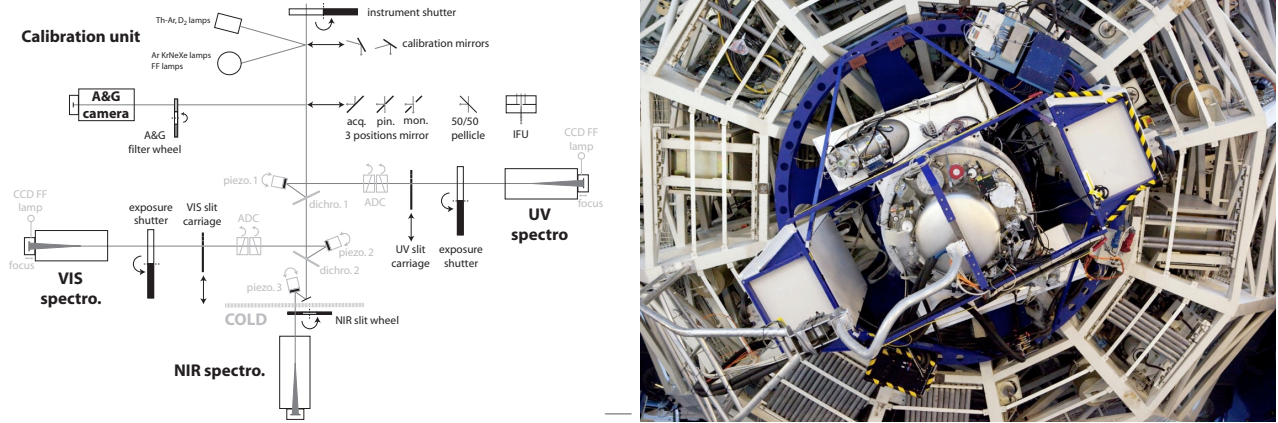


Figure 1. A view of X-shooter at the Cassegrain focus of the VLT UT2.

The Consortium which has built X-shooter consists of 10 institutes in Denmark, France, Italy, The Netherlands and ESO. The instrument has been completed in 5 years at a cost of 7 million Euros and ~ 70 person-years.

Overview of the instrument and details on its design and manufacturing have been included in previous SPIE publications by D’Odorico et al.^{1,2}(Overview), Spano et al.³(Optical design), Kjaergaard-Rasmussen et al.⁴(Backbone, UV-Blue and Visible spectrographs), Navarro et al.^{5,6} (Near-IR spectrograph), Roelfsema et al.⁷ (Cryogenic design), Guinouard et al.⁸ (Integral Field Unit), Vidali et al.⁹ (Control software) and Goldoni et al.¹⁰ (Data reduction software). The present contribution focusses on the instrument performances (resolution, throughput, background, stability) as measured during testing, commissioning and the first months of science operations.

2. SPECTRAL FORMAT AND RESOLUTION

The spectral format of X-shooter is fixed. The whole spectral range is covered by 12 orders in the UVB, 15 in the VIS, and 16 in the NIR. Orders are strongly curved (parabolic) and the spectral line tilt varies along orders. Both slit height and width projection also vary from order to order and along each order due to a variable anamorphic effect introduced by the prisms (crossed twice). The minimum separation between orders is 4 (unbinned) pixels to allow inter-order background evaluation. The dichroic crossover between UVB-VIS and VIS-NIR is at 559.5 nm and 1024 nm respectively, near the location of atmospheric features. Grating line densities were chosen to have the crossovers occur near the ends of the order. The spectral ranges on the detector and blaze wavelength for each order are given in Fig. 2 together with an example of ThAr slit frame for each arm. These measurements are in excellent agreement with the predicted spectral format.³

In terms of image quality and spectral resolution, the three arms of X-shooter perform fully within specifications. Resolution as a function of slit width is given in Fig. 3.

3. EFFICIENCY

Thanks to the very high efficiency of the two dichroics splitting light between the three arms and the careful optimization of each arm, the resulting overall throughput of X-shooter is very high. The efficiency for each order as measured during the last commissioning run using spectro-photometric standard BD+17 4708 is given in Fig. 4. Taking orders individually (not combining signal from different orders), efficiency peaks at 33%, 34% and 31% for the UVB, VIS and NIR arm respectively

The overall efficiency is essentially as predicted by multiplying efficiencies of the different optical elements and detectors except for the J band where it is $\sim 30\%$ below our original goal, due to losses that can only be partly explained by scattering in the ZnSe cross-disperser prisms.

Order	Min. wavelength [nm]	Blaze wavelength [nm]	Max. wavelength [nm]
UVB			
24	293.6	312.2	322.3
23	306.2	325.0	336.2
22	320.0	339.8	351.4
21	335.1	356.1	368.0
20	351.8	373.5	386.2
19	370.1	393.2	406.4
18	390.6	414.5	428.9
17	413.4	438.8	454.0
16	439.1	466.4	482.2
15	468.3	496.8	514.2
14	501.6	531.0	550.8
13	540.1	566.0	593.0
VIS			
30	525.3	550.5	561.0
29	535.8	568.0	580.2
28	554.6	585.9	600.8
27	575.2	607.7	622.9
26	597.4	629.5	646.8
25	621.3	653.8	672.5
24	647.2	682.1	700.4
23	675.4	711.2	730.7
22	706.1	742.6	763.8
21	739.7	777.6	800.0
20	777.0	815.8	839.8
19	817.6	860.2	883.8
18	862.9	904.3	932.7
17	913.7	957.3	987.4
16	970.7	1001.6	1048.9
NIR			
26	982.7	1005.8	1034.2
25	1020.5	1046.0	1076.7
24	1062.0	1089.6	1122.9
23	1106.6	1137.0	1173.1
22	1155.2	1188.6	1228.0
21	1208.2	1245.2	1288.5
20	1266.5	1307.5	1355.2
19	1330.3	1376.3	1429.4
18	1400.8	1452.8	1511.5
17	1479.5	1538.2	1604.0
16	1567.1	1634.4	1708.7
15	1667.8	1743.3	1823.3
14	1785.7	1867.9	1952.8
13	1922.6	2011.5	2102.0
12	2082.9	2179.3	2275.6
11	2272.3	2377.28	2480.7

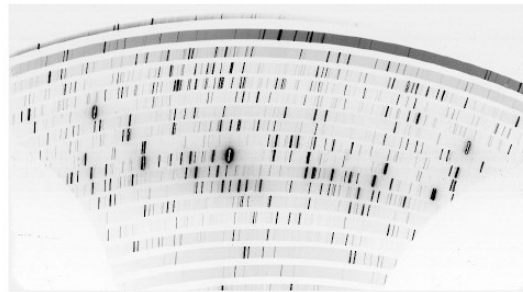
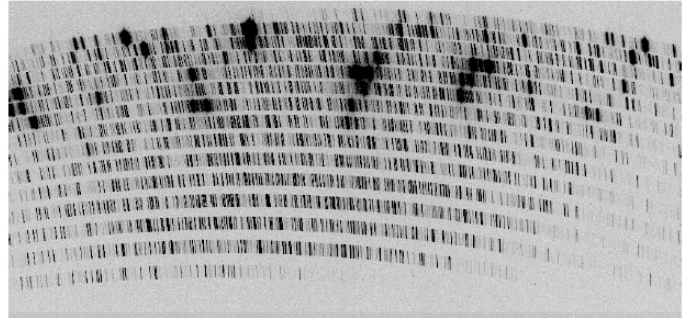
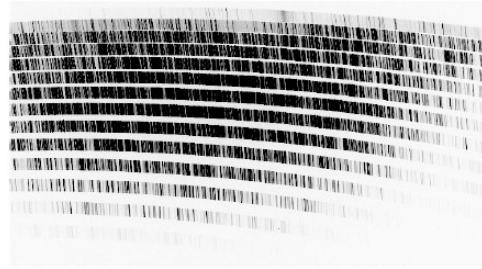


Figure 2. Right: The X-shooter spectral format for the UVB (top), VIS (middle) and NIR (bottom) arm as measured at the telescope. Left: an example of ThAr slit frame for each arm.

Slit width	UVB		Slit width	VIS		Slit width	NIR	
	R $\lambda/\Delta\lambda$	Sampling [pix/FWHM]		R $\lambda/\Delta\lambda$	Sampling [pix/FWHM]		R $\lambda/\Delta\lambda$	Sampling [pix/FWHM]
0.5	9100	3.5	0.4	17400	3.0	0.4	11300	2.0
0.8	6200	5.2	0.7	11000	4.8	0.6	8100	2.8
1.0	5100	6.3	0.9	8800	6.0	0.9	5600	4.0
1.3	4000	8.1	1.2	6700	7.9	1.2	4300	5.3
1.6	3300	9.9	1.5	5400	9.7	1.5	3500	6.6
IFU	7900	4.1	IFU	12600	4.2	IFU	8100	2.8

Figure 3. Measured resolution as a function of slit width.

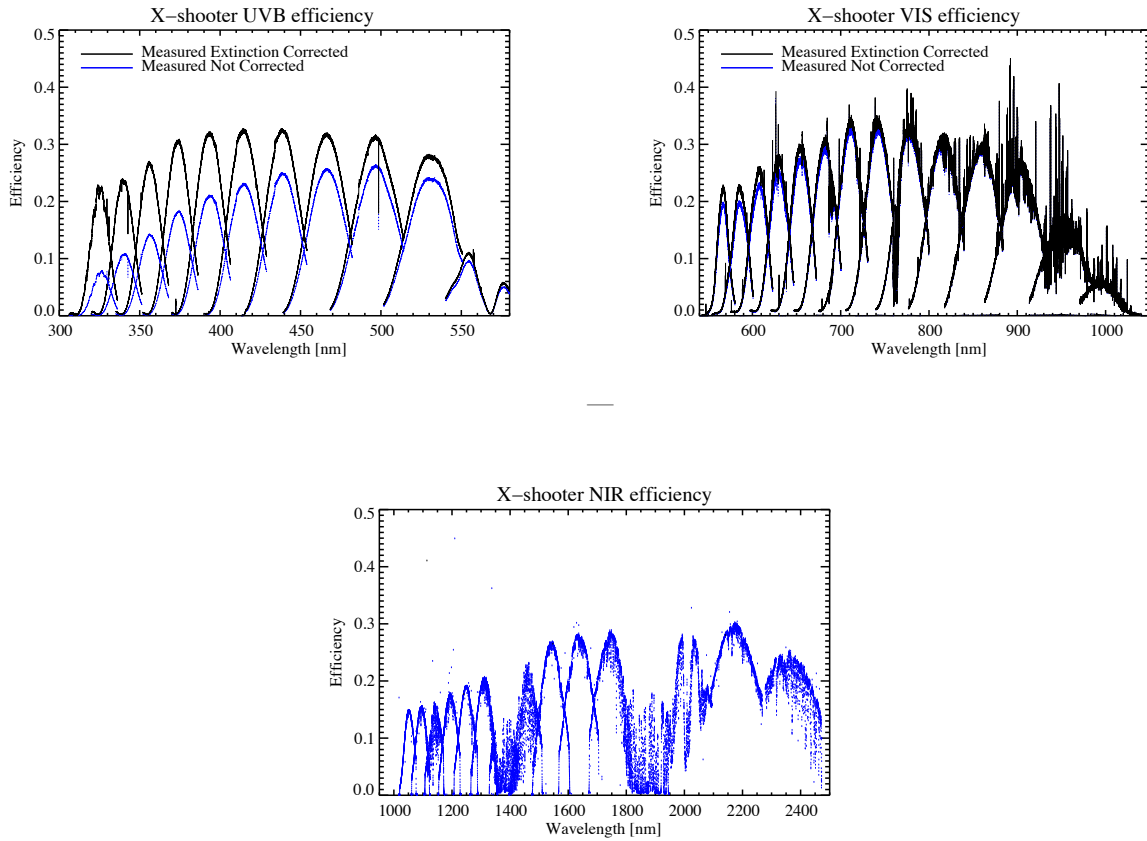


Figure 4. The overall throughput of X-shooter, including telescope, as measured during the last commissioning run in September 2009 using spectrophotometric standard BD+17 4708. Blue curves represents raw measurements and black curves show the efficiency corrected for atmospheric extinction (UVB and VIS only)

4. STABILITY

4.1 Flexures

Being mounted at the Cassegrain focus, X-shooter is subject to changing gravity vector, hence changes in instrument flexures that have to be kept under control. This splits into two components: (i) flexures of the instrument backbone (i.e. before the slit) that affect the relative alignment of the three spectrographs; (ii) flexures within each spectrograph (i.e. after the slit) that mainly affect the quality of the wavelength calibration and the sky subtraction.

4.1.1 Spectrograph flexures

Changes in the spectral format with position have been analyzed in details during integration and testing in Garching and further checked during commissioning in Paranal. Performances at the telescope are shown in Fig. 5. As can be read from panels a and b, flexures induce a simple rigid shift of the spectral format that is $\lesssim 1.15$ pixels in the UVB arm and $\lesssim 1.0$ pixel in the VIS arm. No variation of image quality is measured for those two arms.

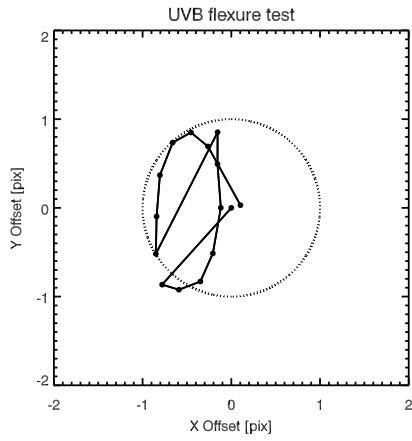
Concerning the NIR arm, behavior is more complex as illustrated in panel c of Fig. 5 which shows the recorded image motion for various calibration lines throughout the spectral format. Compared to their (X, Y) position at zenith, spectral lines move by up to 1.4 pixels. However, this effect is larger on the edges than in the center of the detector hinting to an effect of flexure on image scale. This is possibly due to some small residual motion of the detector which is linked to a heavy copper bar reaching the LN2 tank to maintain its low operating temperature. This hypothesis is further supported by measured variations of the spot FWHM by up to $\sim 15\%$ which however stays well within our image quality specifications.

4.1.2 Active flexure compensation of the backbone

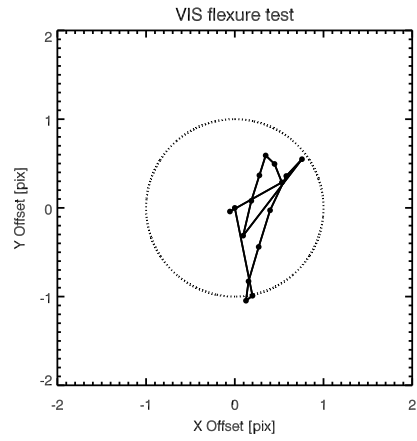
One of the main challenges with the three arm design is to keep the three slits staring at the same patch of sky at any position angle and zenithal distance. In order to always guarantee an alignment to better than 1/10th of the narrowest slit width, X-shooter is equipped with an Active Flexure Compensation (AFC) system: each arm has a piezo mounted folding mirror which is adjusted during each acquisition, immediately after the telescope and the instrument have reached their position for science observations. Flexure measurement is done through the following steps:

1. take simultaneously in the 3 arms an arc spectrum through the 0.5 arcsec pinhole located in the spectrograph slit slide/wheel (Fig. 6a)
2. take a spectrum using a reference 0.5 arcsec pinhole in the Cassegrain focal plane (see Fig. 6b)
3. measure the displacement between the two frames (at the undeviated wavelength of the Atmospheric Dispersion Compensator) using a cross-correlation algorithm
4. send corresponding commands to piezos (Fig. 6c)
5. repeat steps 2 & 3 to check convergence

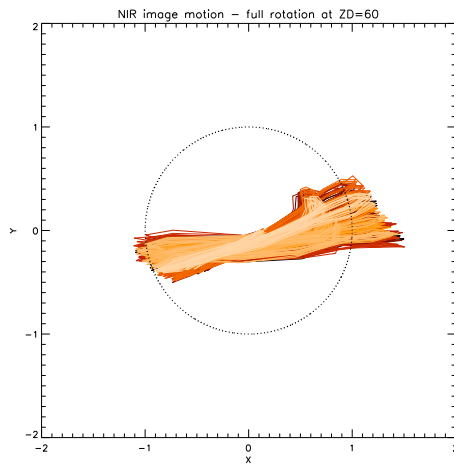
This whole procedure comes at no expenses in terms of overheads since it is done in parallel with the telescope active optics setup. It is operationally very robust and does not require any user interaction. Our measurements show that it reliably maintains the three slits alignment to better than 0.02 arcsec, as illustrated in Fig. 7. As a side product, the first frame of the sequence is actually an “attached” wavelength calibration that is used by the data reduction pipeline to correct the wavelength solution for thermally- and gravity-induced drifts (see Modigliani et al.¹¹).



(a) UVB



(b) VIS



(c) NIR

Figure 5. Measured image position for a full rotation of the instrument at a zenithal distance of 60 deg taking as a reference (0,0) the position measured at zenith. X and Y scales are in pixels. Pixel scale is 0.15 arcsec/pix for UVB and VIS and 0.2 arcsec for the NIR arm. The dotted circle shows our ± 1 pixel flexure specification.

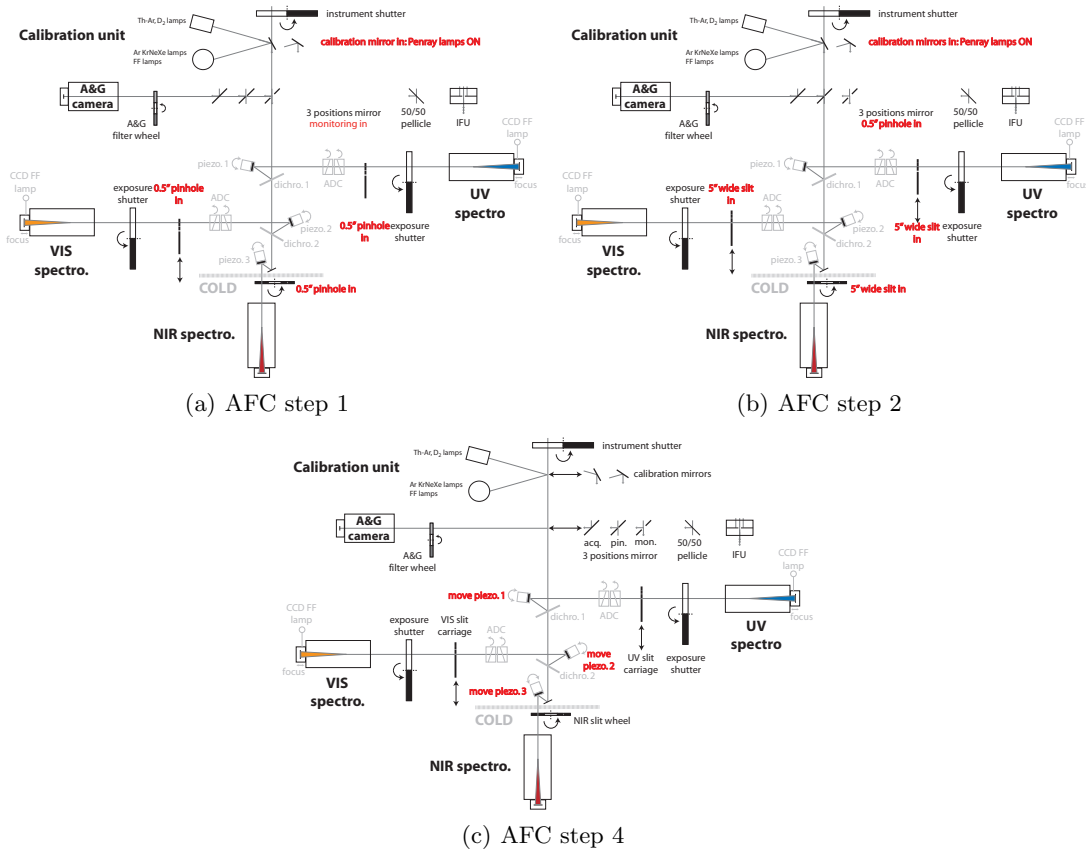


Figure 6. The three steps of the flexure compensation procedure.

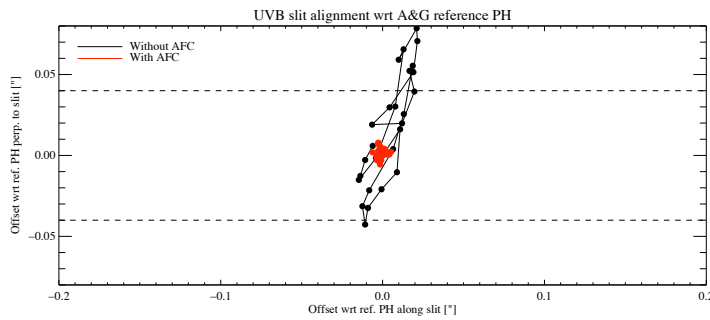


Figure 7. Alignment of the UVB arm 0.5 arcsec pinhole with respect to the focal plane reference pinhole with (red) and without the flexure compensation (black) through a full rotation of X-shooter at a zenithal distance of 60 deg. The AFC allows to maintain the alignment to ~ 0.01 arcsec, well within specification of $1/10$ th of the narrowest slit width.

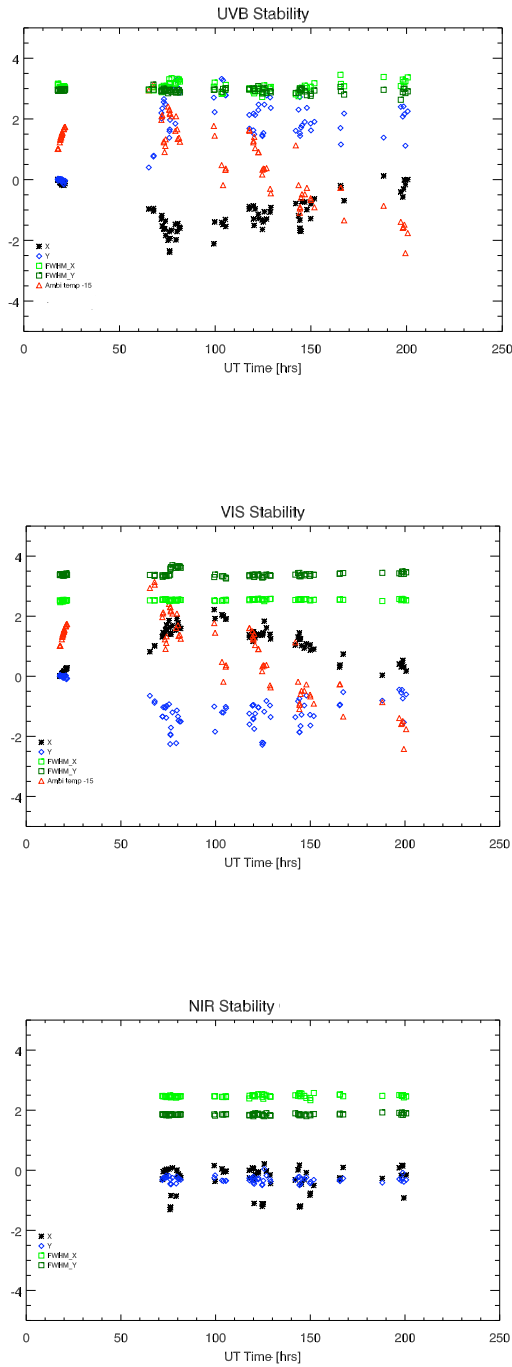


Figure 8. Stability of the UVB (top), VIS (center) and NIR (bottom) spectrograph stability over 6 consecutive nights as measured during the third commissioning run. The dark and light green points show the FWHM in X and Y of a 0.5 arcsec pinhole, the black and blue points show the X and Y position of a reference calibration line with respect to its position measured at zenith on the first day and the red points show the ambient temperature (for UVB and VIS only since it is irrelevant for the temperature controlled NIR arm)

4.2 Overall stability in operations

Flexure measurements presented above represent a rather schematic case of a full rotation of the instrument at 60 deg zenithal distance within a very short time and are not necessarily representative of the actual stability during a scientific observing run where other environmental effects such as temperature can be important. Fig 8 gives one example of monitoring of the instrument stability throughout one commissioning run of X-shooter in March 2009.

Overall, during a given typical night, stability of the spectral format in each arm is stable within ~ 1.5 pix. The most striking global trend is that of the UVB and VIS spectral format drift in the cross dispersion direction ($\sim X$) following the ambient temperature. This behavior is dominated by the change in refractive index of the cross-dispersion prisms which essentially follows predictions at a rate of ~ 0.5 pix/deg. A correlation with temperature is also noticeable in the Y direction (\sim dispersion direction) which can only be partly explained by the fact that the slit image is tilted with respect to the lines and columns of the detector (see spectral format in Fig. 2). Note also that the scatter in image quality visible in the UVB arm is due to an improper camera focus-temperature relation at the time of that particular commissioning run. Since the NIR arm is temperature controlled, its longer term stability appears much higher.

For a more detailed discussion of the long term stability and monitoring based on a physical model of the instrument, please refer to Möhler et al.¹² and Bristow et al.¹³

5. CONCLUSIONS

In this paper, we have presented key figures demonstrating X-shooter's high performances on sky. This unique instrument lives up to expectations in terms high throughput, resolution and exquisite image quality. It is overall a bit less stable than originally targeted but flexures are nevertheless kept within in a very reasonable range ensuring no significant impact on scientific performance. The novel concept developed to compensate for backbone flexures and accurately maintain the three slits staring at the same patch of sky is very efficient and robust in operations.

REFERENCES

- [1] D'Odorico, S., Andersen, M. I., Conconi, P., De Caprio, V., Delabre, B., Di Marcantonio, P., Dekker, H., Downing, M. D., Finger, G., Groot, P., Hanenburg, H. H., Hammer, F., Horville, D., Hjorth, J., Kaper, L., Klougart, J., Kjaergaard-Rasmussen, P., Lizon, J., Marteaud, M., Mazzoleni, R., Michaelsen, N., Pallavicini, R., Rigal, F., Santin, P., Norup Soerensen, A., Spano, P., Venema, L., Vola, P., and Zerbi, F. M., "X-shooter: UV-to-IR intermediate-resolution high-efficiency spectrograph for the ESO VLT," *SPIE Conference Series* **5492**, 220–229 (Sept. 2004).
- [2] D'Odorico, S., Dekker, H., Mazzoleni, R., Vernet, J., Guinouard, I., Groot, P., Hammer, F., Rasmussen, P. K., Kaper, L., Navarro, R., Pallavicini, R., Peroux, C., and Zerbi, F. M., "X-shooter UV- to K-band intermediate-resolution high-efficiency spectrograph for the VLT: status report at the final design review," *SPIE Conference Series* **6269** (July 2006).
- [3] Spanò, P., Delabre, B., Norup Sørensen, A., Rigal, F., de Ugarte Postigo, A., Mazzoleni, R., Sacco, G., Conconi, P., De Caprio, V., and Michaelsen, N., "The optical design of the X-shooter for the VLT," *SPIE Conference Series* **6269** (July 2006).
- [4] Rasmussen, P. K., Zerbi, F. M., Dekker, H., Vernet, J., Andersen, J. J., De Caprio, V., Dimarcantonio, P., D'Odorico, S., Lizon, J., Lucuix, C., Michaelsen, N., Molinari, E., Nørregaard, P., Riva, A., Riva, M., Santin, P., Sørensen, A. N., Spanò, P., and Wistisen, D., "X-shooter-backbone and UV-blue and visible spectrographs: final AIV and measured performances," *SPIE Conference Series* **7014** (Aug. 2008).
- [5] Navarro, R., Elswijk, E., de Haan, M., Hanenburg, H., ter Horst, R., Kleszcz, P., Kragt, J., Pragt, J., Rigal, F., Roelfsema, R., Schoenmaker, T., Tromp, N., Venema, L., Groot, P., and Kaper, L., "X-shooter near-IR spectrograph arm: design and manufacturing methods," *SPIE Conference Series* **6273** (July 2006).
- [6] Navarro, R., Elswijk, E., Tromp, N., ter Horst, R., Horrobin, M., Vernet, J., Finger, G., Groot, P., and Kaper, L., "X-shooter near-IR spectrograph arm realisation," *SPIE Conference Series* **7014** (Aug. 2008).

- [7] Roelfsema, R., Albers, P., Lizon, J., van Dael, P., Elswijk, E., Groot, P., Hanenburg, H., Kragt, J., Navarro, R., Tromp, N., and Wulterkens, G., “X-shooter near infra-red spectrograph cryogenic design,” *SPIE Conference Series* **7017** (July 2008).
- [8] Guinouard, I., Horville, D., Puech, M., Hammer, F., Amans, J., Chemla, F., Dekker, H., and Mazzoleni, R., “An integral field unit for X-shooter,” *SPIE Conference Series* **6273** (July 2006).
- [9] Vidali, M., Di Marcantonio, P., Santin, P., Vernet, J., and Zacchei, A., “The ESO-VLT X-SHOOTER instrument software in the VLT environment,” *SPIE Conference Series* **6274** (July 2006).
- [10] Goldoni, P., Royer, F., François, P., Horrobin, M., Blanc, G., Vernet, J., Modigliani, A., and Larsen, J., “Data reduction software of the X-shooter spectrograph,” *SPIE Conference Series* **6269** (July 2006).
- [11] Modigliani, A., Goldoni, P., Royer, F., Haigron, R., Guglielmi, L., François, P., Horrobin, M., Bristow, P., Vernet, J., Moehler, S., Kerber, F., Ballester, P., Mason, E., and Christensen, L., “The X-shooter pipeline,” *SPIE conference series* (2010).
- [12] Moehler, S., Bristow, P., Kerber, F., Modigliani, A., and Vernet, J., “The physical model in action: Quality control for x-shooter,” *SPIE Conference Series* (2010).
- [13] Bristow, P., Vernet, J., Kerber, F., Moehler, S., and Modigliani, A., “Using the x-shooter physical model to understand instrument flexure,” *SPIE conference Series* **7735**(271) (2010).